Effect of isolation pads and their stiffness on the dynamic characteristics of bridges

W. Dai[a,*], M.O. Moroni[b], J.M. Roesset[c], M. Sarrazin[b]

[a] *12750 Merit Drive, Suite 750, LB-7, Dallas, TX 75251-1226, United States*
[b] *University of Chile, Blanco Encalada 2002, Santiago, Chile*
[c] *Texas A&M University, TAMU-3136, College Station, TX 77843-3136, United States*

Abstract

In this paper, the effect of the stiffness of the rubber pads on the dynamic characteristics of a base-isolated bridge is examined using transfer functions in the frequency domain. A three dimensional structural model that accounts for continuous mass distribution along each member is used. Results are obtained for a model of the bridge without isolation pads and for various values of the shear modulus of the rubber. This allows comparing the values of the predominant frequencies and the dynamic amplification of the motions over an extended range of frequencies. The results are then compared to the power spectra of the motions recorded at three points of an instrumented pier (the base, the top of the pier, and the same location on the deck) under an actual earthquake. The model can explain some of the observed behavior very well although there are still some points that cannot be resolved due to lack of sufficient information on the spatial variability of the motions.

Keywords: Base isolation; Rubber pads; Frequency domain; Continuous mass distribution; Transfer functions

1. Introduction

Base isolation is now accepted and recognized worldwide as an effective method to reduce the seismic demand on structures and there are already some excellent books related to the design of base-isolated systems [1,2]. The approach has been extensively used for buildings in the United States, Japan, New Zealand and Italy, with excellent results under strong ground motions. The application to bridges was a logical step, because bridges already have in most cases horizontal stiffness bearings that allow thermal deformations of the deck. The use of multi-layer elastomeric bearings for seismic protection was thus a natural extension of the rubber pads used for thermal expansion. A large number of studies have been conducted over the last 15 years to investigate the adequacy of various types of isolation pads, their material properties and behavior under different environmental conditions, and the effect of their properties on the seismic response of a bridge [3–9]. In this paper we evaluate the application to a specific structure, the Marga–Marga Bridge, near Viña del Mar, in the central coastal region of Chile. This bridge, built in 1996, was instrumented with 21 accelerometers distributed over the deck, along one pier, and in the free field. A number of earthquakes have been recorded by these instruments, including one, on July 24, 2001, with peak ground acceleration in the free field of $0.2g$ in the longitudinal direction of the bridge, over $0.1g$ in the transverse direction and $0.05g$ vertically. The existence of these data and results of ambient vibration tests conducted immediately after completion of the construction provide a unique opportunity to evaluate the accuracy of different analytical models of the structure and our capacity to predict the observed behavior. Students at the University of Chile under the supervision of two of the authors (Moroni and Sarrazin) have been conducting research on base isolation in general and on the behavior of the Marga–Marga bridge in particular, for the last ten years, using different structural models and interpreting the recorded data. The work described in this paper is an extension of their research effort.

* Corresponding author.
E-mail address: daiwentao@gmail.com (W. Dai).

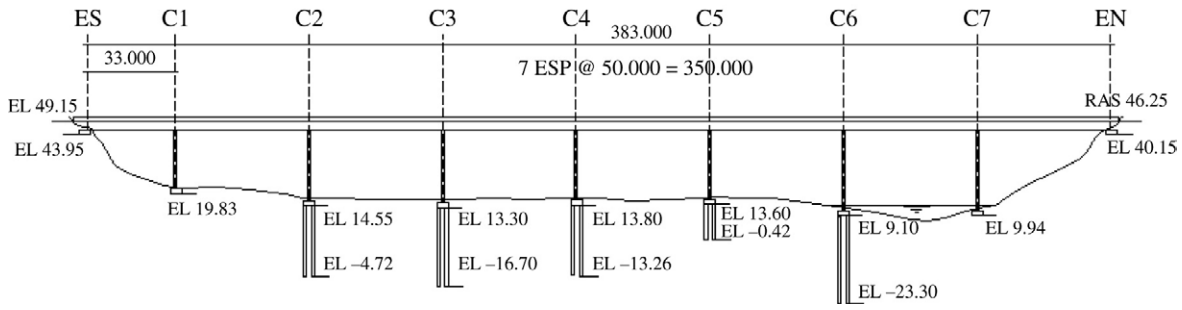

Fig. 1. Overview of Marga–Marga bridge.

2. Structural model

The Marga–Marga bridge is shown schematically in Fig. 1. The deck consists of eight spans, all 50 m long except for the span connecting the south abutment and pier 1, which is 33 m long. The deck is composite with a concrete slab over four steel I-beams. It was modeled as an equivalent beam with a mass density, Poisson's ratio and Young's modulus of 2940 kg/m^3, 0.245 and 3.3 $\times$ 10^{10} Pa, respectively. The centroid of the equivalent beam cross section is 2.65 m above the top of the base isolators (rubber pads) and 0.45 m below the upper surface (as shown in Fig. 2). The properties of the deck cross section are:

$$\begin{cases} A = 8.13(\mathrm{m}^2),\ A_{sy} = 3.85(\mathrm{m}^2),\ A_{sz} = 2.25(\mathrm{m}^2) \\ I_z = 238.6(\mathrm{m}^4),\ I_y = 5.98(\mathrm{m}^4),\ J = 0.116(\mathrm{m}^4) \end{cases}$$

in which A is the area of the deck's cross section; A_{sy} and A_{sz} are the effective shear areas of the composite cross section in the Y (transverse) and Z (vertical) direction, respectively; I_z and I_y are the bending moments of inertia in the Z and Y direction, respectively, and J is the torsional moment of inertia.

The piers and their dimensions are illustrated in Fig. 3. The formulation used assumes a constant cross section for each member. Each pier was therefore divided into three members according to the variation of the cross section. As shown in Figs. 3 and 4, the top and bottom parts (members) are solid, while the long member in between is hollow. The mass density, Poisson's ratio and Young's modulus used in the analysis for the piers are 2500 kg/m^3, 0.2 and 3.3 $\times$ 10^{10} Pa, respectively. The properties of the pier cross sections are:

$$\begin{cases} A = 31.6(\mathrm{m}^2),\ A_{sy} = 26.86(\mathrm{m}^2) \\ I_x = 657.385(\mathrm{m}^4),\ A_{sx} = 26.86(\mathrm{m}^2) \\ I_y = 10.533(\mathrm{m}^4),\ J = 37.92(\mathrm{m}^4) \end{cases} \quad \text{and}$$

$$\begin{cases} A = 6.38(\mathrm{m}^2),\ A_{sy} = 4.17(\mathrm{m}^2) \\ I_x = 63.33(\mathrm{m}^4),\ A_{sx} = 1.25(\mathrm{m}^2) \\ I_y = 4.18(\mathrm{m}^4),\ J = 12.658(\mathrm{m}^4) \end{cases}$$

for the top member and the middle member, respectively. The properties of the bottom members' cross sections are:

$$\begin{cases} A = 74.25(\mathrm{m}^2),\ A_{sy} = 63.113(\mathrm{m}^2) \\ I_x = 1127.672(\mathrm{m}^4),\ A_{sx} = 63.113(\mathrm{m}^2) \\ I_y = 187.172(\mathrm{m}^4),\ J = 552.531(\mathrm{m}^4) \end{cases} \quad \text{and}$$

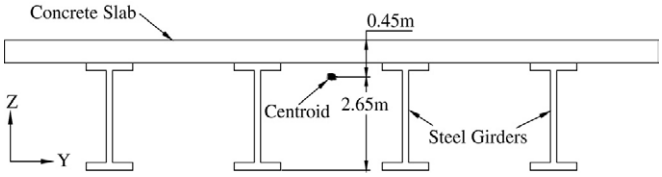

Fig. 2. Cross section of deck.

$$\begin{cases} A = 57.75(\mathrm{m}^2),\ A_{sy} = 49.088(\mathrm{m}^2) \\ I_x = 530.578(\mathrm{m}^4),\ A_{sx} = 49.088(\mathrm{m}^2) \\ I_y = 145.578(\mathrm{m}^4),\ J = 396.555(\mathrm{m}^4) \end{cases}$$

for piers 2–6 and piers 1 & 7, respectively, where A_{sx} is the shear area in the X (longitudinal) direction and I_x is the bending moment of inertia around the X axis.

The rubber pads in the structure act as base isolators to mitigate the motion of the deck due to earthquakes. On the top of each pier, four rubber pads (each under one of the four steel I-beams) were placed in a line, separately, along the Y axis, as shown in Fig. 5. They were combined into one structural member in the analysis.

The rubber pads were made of alternating layers of rubber and steel, so they have a relatively high axial stiffness and lower shear stiffness. To model this, equivalent Young's modulus, E_{eqvl} and shear modulus, G_{eqvl} were selected to match the axial and shear stiffness according to

$$\begin{cases} K_V = \dfrac{1}{\sum\limits_i \frac{L_i}{E_i A}} = \dfrac{E_{\mathrm{eqvl}} A}{\sum\limits_i L_i} \\ K_H = \dfrac{1}{\sum\limits_j \frac{L_j}{G_j A_s}} = \dfrac{G_{\mathrm{eqvl}} A_s}{\sum\limits_j L_j} \end{cases}$$

where E_k, G_k and L_k represent the Young's modulus, shear modulus and thickness of the kth layer; A and A_s are the area and shear area of the cross section; i denotes all rubber and steel layers while j only denotes the rubber layers.

Rubber is a non-linear material, so E_k and G_k of the rubber pads actually depend on the magnitude of the deformation. Daza [12] suggested a variation of the shear modulus with shear strain given by $G = 6.0 \times 10^5 \cdot \gamma^{-0.3764}$. The length of the rubber pad members is 0.2 m and the mass density is 3000 kg/m^3. The cross section properties of the rubber pad members are summarized as:

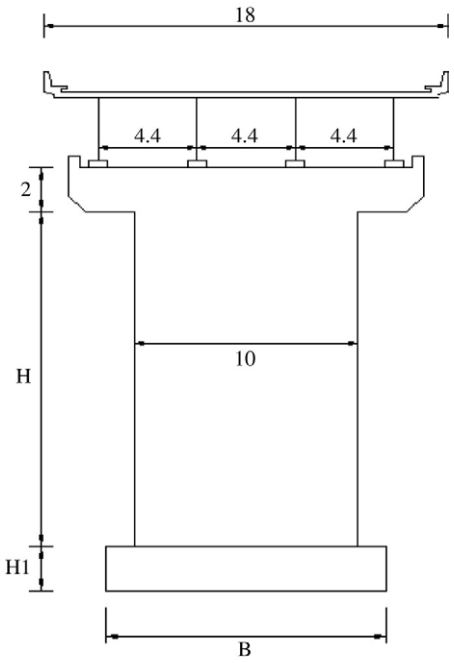

Pier #	H (m)	H1 (m)	B (m)
1	21.865	1.5	10.5
2	26.317	2.0	13.5
3	27.138	2.0	13.5
4	26.260	2.0	13.5
5	26.082	2.0	13.5
6	30.154	2.0	13.5
7	30.086	1.5	10.5

Fig. 3. Transverse view of pier and its dimensions.

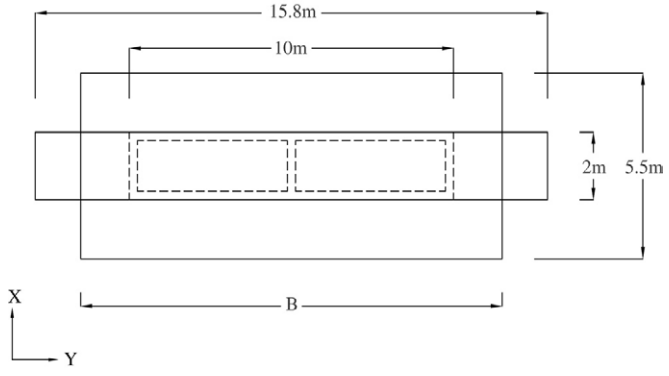

Fig. 4. Cross sections of pier.

$$\begin{cases} A = 1.738(\mathrm{m}^2) \\ A_{sy} = 1.477(\mathrm{m}^2) \\ I_x = 168.269(\mathrm{m}^4) \\ A_{sx} = 1.477(\mathrm{m}^2) \\ I_y = 0.099(\mathrm{m}^4) \\ J = 35.845(\mathrm{m}^4) \end{cases}, \quad \begin{cases} A = 0.906(\mathrm{m}^2) \\ A_{sy} = 0.770(\mathrm{m}^2) \\ I_x = 87.747(\mathrm{m}^4) \\ A_{sx} = 0.770(\mathrm{m}^2) \\ I_y = 0.017(\mathrm{m}^4) \\ J = 18.672(\mathrm{m}^4) \end{cases} \quad \text{and}$$

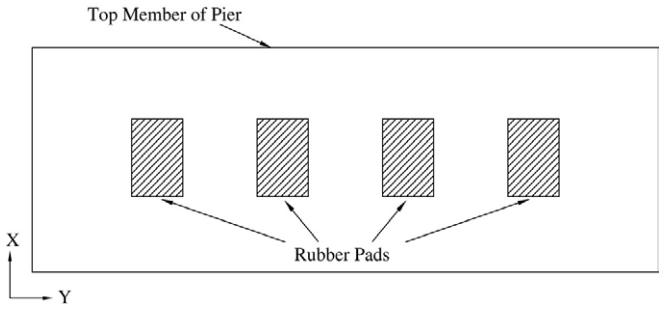

Fig. 5. Rubber pads on top of pier.

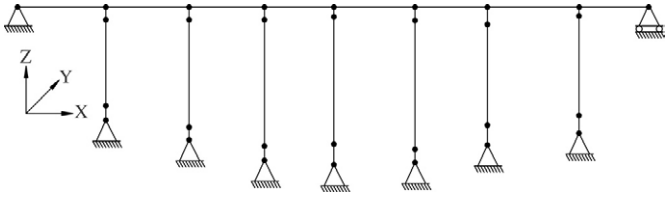

Fig. 6. Structural model (without rubber pads).

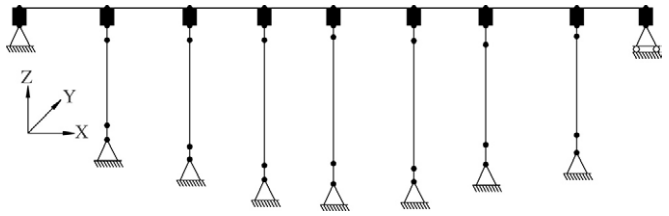

Fig. 7. Structural model (with rubber pads, free deck).

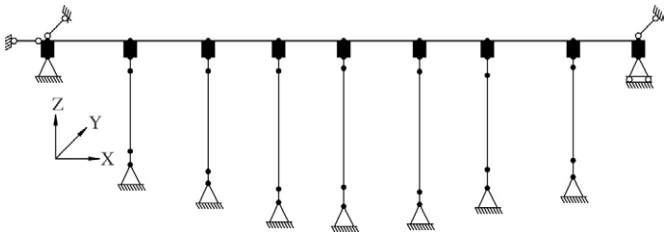

Fig. 8. Structural model (with rubber pads, constrained deck).

$$\begin{cases} A = 1.109(\mathrm{m}^2) \\ A_{sy} = 0.943(\mathrm{m}^2) \\ I_x = 107.387(\mathrm{m}^4) \\ A_{sx} = 0.943(\mathrm{m}^2) \\ I_y = 0.037(\mathrm{m}^4) \\ J = 22.856(\mathrm{m}^4) \end{cases}$$

for rubber pads on top of the piers, at the north abutment and at the south abutment, respectively.

Figs. 6–8 show the models used in this work. In the constrained deck model (Fig. 8), the deck is constrained in both X and Y directions at the left end and only in the Y direction at the right end.

3. Formulation

The studies previously conducted at the University of Chile used well known computer programs such as SAP with linear

Table 1
Natural frequencies of Marga–Marga bridge from former studies (Hz)

		Longitudinal				Transverse				Vertical			
Experimental data 1	May 1996	1.86				1.17	1.42	2.1					
Experimental data 2	July 1996	1.71				1.07	1.27	1.9					
Segovia [10]	No rubber pads	3.85				2	2.22	2.7					
	5% deformation	1.54				0.71	1.02	1.85					
Romo [11]	No rubber pads	2.01	2.13	2.39	2.77	1.29	1.79	2.67	3.36				
	Free deck	0.65	2.09	2.24		0.93	2.18		1.87				
	Constrained deck	2.01	2.03	2.1	2.25	0.93	1.28	2.18					
Daza [12]		0.67	2.5	2.8		0.96	1.5		1.88	2.1	2.56		

members and in some cases shell finite elements (plate elements in space with stretching and bending) to model the deck and the steel girders. The analyses were conducted in the time domain determining first the natural frequencies and the mode shapes. Table 1 summarizes some of the results of these studies. Romo [11] considered a case with both ends of the deck free in the longitudinal direction and another with the deck constrained at one end in this direction. Daza [12] assumed instead the existence of a longitudinal spring at one end to provide only a limited constraint.

In this work the analyses were conducted in the frequency domain determining the transfer functions for the motions (accelerations, velocities or displacements) at various points (locations of the recording instruments) due to unit harmonic motions at the base of each pier. These transfer functions could then be combined to reproduce different motions for each pier, but the lack of information on what these motions might have been limited the studies to the case where all supports move in phase. The peaks of the transfer functions correspond to the natural frequencies but only for those modes that will be excited. The transfer functions select therefore the significant modes from the point of view of the response to an earthquake with the same motion at all supports.

The model of the bridge used to obtain the transfer functions is a three dimensional frame with distributed masses (in contrast to concentrated or consistent masses). The dynamic stiffness matrices in the frequency domain for linear structural members with distributed masses were first used by Latona [13] to validate the accuracy of lumped and consistent mass matrices. Formulations for beam members and shell elements were then obtained by Kolousěk [14], Banerjee and William [15–17], Doyle [18,19], Papaleontiou [20], Gopalakrishnan and Doyle [21] and Yu and Roësset [22]. In this work the dynamic stiffness matrices with distributed masses were used, extending the formulation of Yu and Roësset [22] to include shear deformation, rotatory inertia and the effect of axial forces [23].

4. Results

4.1. Longitudinal direction (X direction)

Figs. 9 and 10 show the transfer functions of the motions on the deck and on top of pier 4 due to a unit harmonic motion in the longitudinal direction (X direction) at the bottom of all piers.

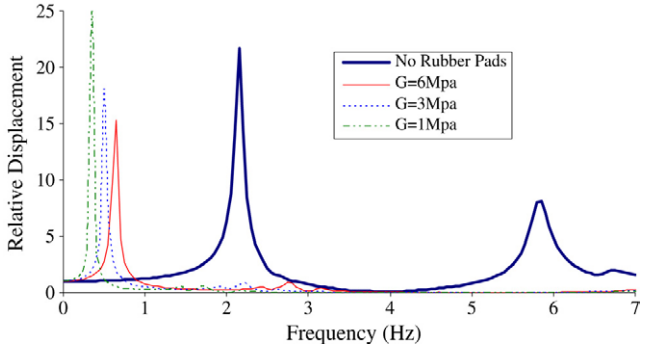

Fig. 9. Comparison of displacements at the deck in the X direction due to a unit motion at the bases of all piles (free deck).

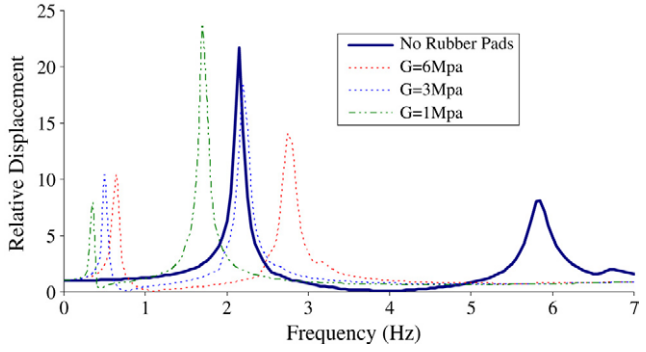

Fig. 10. Comparison of displacements at top of pier in the X direction due to a unit motion at the bases of all piles (free deck).

It can be seen that, in the longitudinal direction, without rubber pads, the first two significant peaks of the transfer function due to the same unit harmonic base motion at all piers occur at 2.15 Hz and 5.85 Hz, respectively. The first peak occurs at a frequency very similar to that of the first two modes reported by Romo (2.01 and 2.13 Hz) for the same case.

The rubber pads will change the frequency response characteristics of the structure. The equivalent shear modulus of the rubber pads is 6.0 MPa, which corresponds to a shear deformation of 0.23% according to the result of a regression analysis of experimental data reported by Daza [12]. It can be seen that the frequencies at the first two significant peaks have been reduced to 0.65 and 2.75 Hz. It should be noted that the amplitude of the peak at 0.65 Hz is larger for the motion of the deck than for that on top of the pier, whereas at 2.75 Hz, the displacement of the deck has been greatly reduced compared

Table 2
Effect of rubber pads' stiffness on longitudinal natural frequencies with free deck (Hz)

G of rubber pads (10^6 Pa)	1st longitudinal	2nd longitudinal	3rd longitudinal	4th longitudinal	5th longitudinal
1	0.35*	1.45	1.7*	2.15	9.55*
1.8	0.45	1.65	1.95	2.35	9.65
3	0.5*	1.95	2.2*	2.6	9.75*
4	0.55	2.1	2.4	2.8	9.85
5	0.6	2.3	2.6	3	9.9
6	0.65*	2.45	2.75*	3.15	10*
7	0.65	2.55	2.92	3.3	
8	0.7		3.05	3.45	
9	0.7		3.2	3.55	
10	0.75		3.35	3.7	

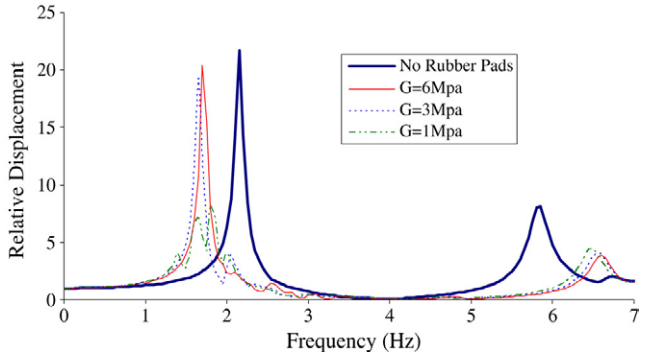

Fig. 11. Comparison of displacements at the deck in the X direction due to a unit motion at the bases of all piles (constrained deck).

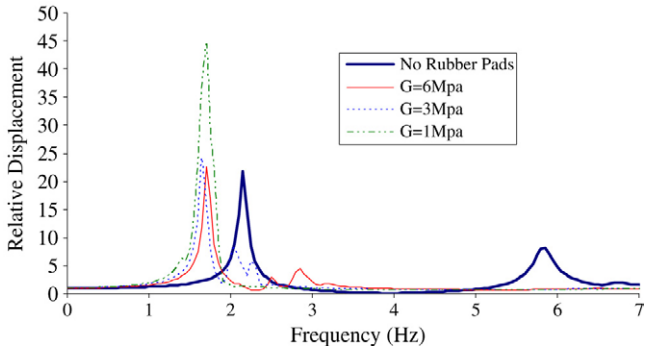

Fig. 12. Comparison of displacements at the top of pier in the X direction due to a unit motion at the bases of all piles (constrained deck).

with that on top of the pier, showing the effect of the rubber pads. There are some small peaks at 2.45 Hz (for the deck) and at 3.15 Hz (both deck and top of pier) but they are not very significant. The frequency of the first significant peak agrees well with the first natural frequency reported by both Daza and Romo for a free deck. The second small peak for the deck at 2.45 Hz and the main peak at 2.75 Hz occur at frequencies very similar to those reported by Daza (2.5 and 2.8 Hz).

For the rubber pads with a shear modulus of 3.0 and 1.0 MPa, the first two significant peaks occur now at 0.50 Hz, 2.20 Hz and 0.35 Hz, 1.70 Hz, respectively. The displacements of the deck are always smaller than those on top of the pier for all frequencies except at the first peak.

The frequencies of all the peaks observed in the transfer functions are listed in Table 2 for the range of the shear modulus of the pads from 1 to 10 MPa. It should be noted again that some of these peaks are very small. The most significant peaks are marked with an asterisk for the three cases shown in Figs. 9 and 10.

In all these cases it was assumed that the deck was free to displace at the ends on top of the rubber pads. A more realistic assumption is that the motions of the ends of the deck are partly prevented. The results obtained on fixing the left end of the deck in the longitudinal direction are shown in Figs. 11 and 12. The true situation is likely to be somewhere in between these two extreme cases, but to reproduce it better it would be necessary to have additional information on the characteristics of the soil (rock) behind the abutments, data that were not available.

For the case of rubber pads with a shear modulus of 6.0 MPa and a constrained deck, the first significant peak occurs at 1.7 Hz (rather than the 0.65 Hz for a free deck). This value agrees well with experimental data from ambient vibration. It is followed by two small peaks at 2.5 and 2.85 Hz at the top of pier 4. The motion of the deck would be apparently amplified at 6.5 Hz in this case.

For rubber pads with a shear modulus of 3.0 and 1.0 MPa, the transfer functions of the motions both on the deck and on top of the pier have several peaks between 1.5 and 2.0 Hz. The peaks for other values of the rubber pads' shear modulus with a constrained deck are listed in Table 3. The significant peaks for the three cases shown in Figs. 11 and 12 are again identified by an asterisk.

Fig. 13 shows the power spectra (square of the amplitude Fourier spectra of the motions) recorded on the Marga–Marga bridge in the longitudinal direction under an earthquake that occurred on July 24, 2001. In this figure, the motion at the bottom of pier 4 is labeled as sensor 1, the motion at the top of pier 4 corresponds to sensor 4, and the motion on top of the deck is from sensor 7.

The experimental data show:

(a) A significant peak at about 1.5 Hz in the base motion of the pier, which is considerably reduced on top of the pier and on the deck (the square of the amplitude is 1.5×10^8 at the base, 2.0×10^7 at the top of the pier and 6.0×10^6 on the deck (a reduction in amplitude by factors of $\sqrt{7.5} = 2.74$ at the top of the pier and $\sqrt{25} = 5.0$ on the deck);

Table 3
Effect of rubber pads' stiffness on longitudinal natural frequencies with constrained deck (Hz)

G of rubber pads (10^6 Pa)	1st longitudinal	2nd longitudinal	3rd longitudinal	4th longitudinal	5th longitudinal	6th longitudinal
1	1.4*	1.7	1.8	2	6.5*	9.55*
1.8	1.55	1.8	1.9	2.05	6.5	9.65
3	1.65*	2.05	2.2	2.25	6.55*	9.75*
4	1.7	2.2	2.4	2.5	6.55	9.85
5	1.7	2.35	2.55	2.65	6.6	9.9
6	1.7*	2.5	2.7	2.85	6.6*	9.95*
7	1.75	2.7	2.85	2.95	6.6	10
8	1.75	2.8	3	3.15	6.6	
9	1.75	2.9	3.1	3.25	6.65	
10	1.75	3	3.25	3.4	6.65	

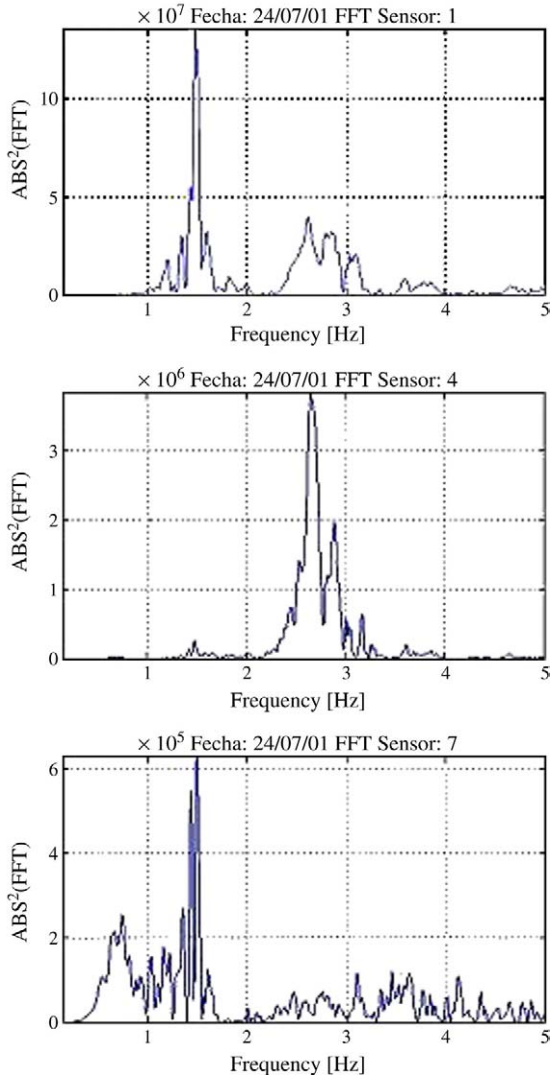

Fig. 13. FFT of recorded longitudinal (X) motion of Marga–Marga bridge during the earthquake of July 24, 2001.

(b) A significant amplification at about 2.7 Hz on top of the pier, which is not present on the deck (the amplification ratio of the amplitude is about $\sqrt{(4\times10^8)/(4\times10^7)}\approx 3.2$ from the base to the top of the pier). The amplitude at the base of the pier at this frequency was slightly smaller than in the free field.

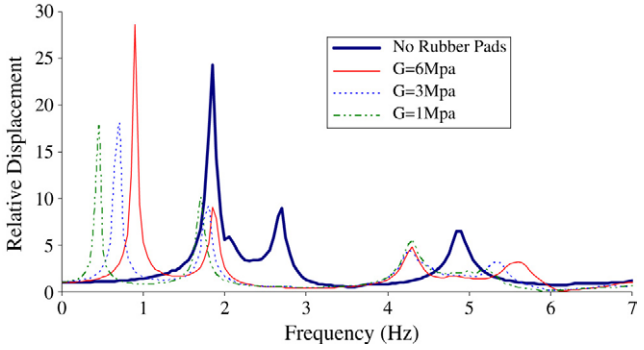

Fig. 14. Comparison of displacements at the deck in the Y direction due to a unit motion at the bases of all piles (constrained deck).

The first natural frequency in shear of the soil deposit itself from a one dimensional soil amplification analysis is about 1.4 Hz, which explains the peak at about 1.5 Hz in the base motion of the pier. As for the amplification at 2.7 Hz, one can find from Figs. 9–12 that this is a natural frequency of the structure. The motion at the top of pier 4 is amplified by a factor of about 4 in Fig. 12. This suggests an effective value of the shear modulus of the rubber pads of about 6.0 MPa.

4.2. *Transverse direction (Y direction)*

In the transverse direction, without rubber pads, the first three significant peaks would be at 1.85 Hz, 2.70 Hz and 4.90 Hz, respectively, as shown in Figs. 14 and 15, which illustrate the transfer function of the motion on top of pier 4 due to a unit harmonic motion in the transverse direction at the bottoms of all the piers. The frequencies of the first two significant peaks are in relatively good agreement with those of the second and third mode in Romo's model for the same case (1.79 and 2.67 Hz), but the peak at about 1.3 Hz that would correspond to his first natural frequency (1.29 Hz) is extremely small, suggesting that the mode is not excited when all supports have the same motion.

For the rubber pads with a shear modules 6.0 MPa and a constrained deck (the deck was always assumed to be constrained transversely at the two ends), it can be seen that the motion of the deck has a significant peak at 0.90 Hz and two small peaks at 1.85 Hz and 4.30 Hz, while the motion of the top of the pier has a significant peak at 5.7 Hz and small ones at 0.9 Hz and 1.85 Hz, as shown in Figs. 14 and 15.

Table 4
Effect of rubber pads' stiffness on transverse natural frequencies (Hz)

G of rubber pads (10^6 Pa)	1st transverse	2nd transverse	3rd transverse	4th transverse	5th transverse
1	0.45*	1.7*	4.3*	5.2*	7.6*
1.8	0.55	1.75	4.3	5.25	7.6
3	0.7*	1.8*	4.25*	5.35*	7.65*
4	0.75	1.8	4.3	5.45	7.65
5	0.85	1.85	4.3	5.5	7.7
6	0.9*	1.85*	4.3*	5.65*	7.7*
7	0.95	1.9	4.3	5.7	7.73
8	1	1.9	4.3	5.8	7.75
9	1.05	1.95	4.3	5.85	7.75
10	1.05	1.95	4.3	5.9	7.8

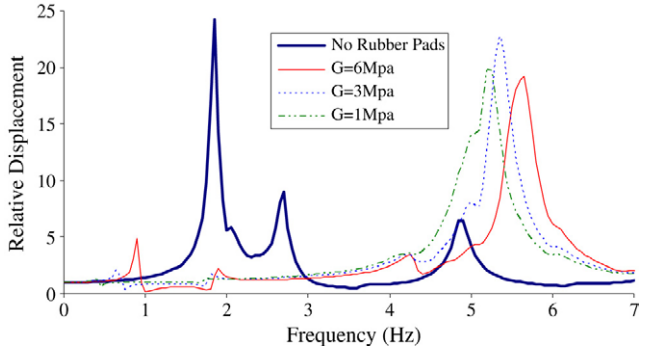

Fig. 15. Comparison of displacements at the top of pier in the Y direction due to a unit motion at the bases of all piles (constrained deck).

The frequency of the first peak is in relatively good agreement with the results of Romo and Daza (0.93 and 0.96 Hz) but no peaks are observed at 1.28 or 1.5 Hz as in their work. Table 4 lists the frequencies of the peaks for different values of the shear modulus.

From the recorded data in the transverse direction shown in Fig. 16, one can observe:

(a) A peak at about 1.3 Hz at the base of the pier with an amplitude squared of 7.5×10^7. It is only 4.0×10^7 at the top of the pier and 2.0×10^7 on the deck, a reduction in amplitude by factors of $\sqrt{7.5/4.0} \approx 1.37$ at the top of the pier and $\sqrt{7.5/2.5} \approx 1.73$ on the deck;
(b) A number of small peaks around 1.0 Hz and a more significant peak at 1.5 or 1.6 Hz on the deck motions with an amplitude squared of 1.5×10^8. This represents an amplification of about $\sqrt{15.0/1.5} \approx 3.2$. This peak is not present on the motion on top of the pier;
(c) A peak at the base and on top of the pier at about 2.7–2.9 Hz, with amplification ratios with respect to the motion at the bottom of the pier of $\sqrt{24/11} \approx 1.50$ for the top of the pier, while the motion is greatly de-amplified on the deck with a ratio of $\sqrt{2/11} \approx 0.43$.

The peak in the base motion at 1.3 Hz is also very close to the shear natural frequency of the soil deposit but the data would suggest that the resonant frequency for the soils is not the same in the longitudinal and the transverse directions of the bridge, an observation which is consistent with the topography of the area. Figs. 14 and 15 show that the structure has a natural frequency at about 1.7–1.85 Hz, where the motion of the deck is greatly

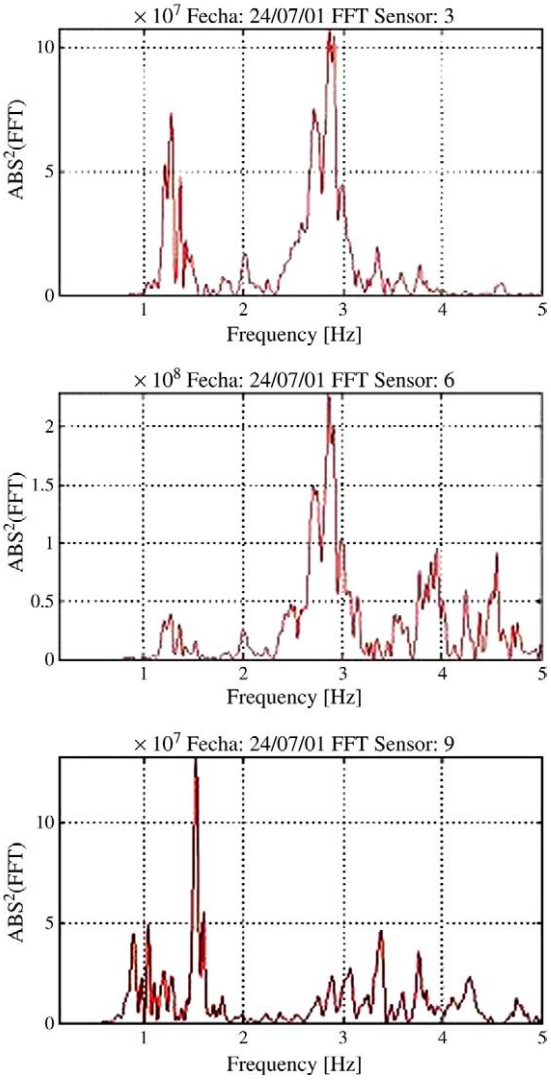

Fig. 16. FFT of recorded transverse (Y) motion of Marga–Marga bridge during the earthquake of July 24, 2001.

amplified, but the base motion has very small amplitudes at these frequencies. At a frequency of 1.5–1.6 Hz, the transfer functions in Figs. 14 and 15 indicate an amplification by a factor of about 2.5–3.0 on the deck and a de-amplification on top of the pier. At 2.7–2.9 Hz, one can calculate that the amplification ratio of the motion from the bottom of the pier

to the top of the pier is about 2.0 and to the deck about 0.3, depending on the stiffness of the rubber pads. While these values do not coincide exactly with the experimental data, they follow the same general trend. It should be noticed that the amplification values will depend on the assumed values of damping.

5. Conclusions

The studies carried out indicate that:

(1) The presence of the isolation pads reduces considerably the amplitude of the longitudinal deck motions with respect to those at top of the pier except at the first natural frequency of the system, which varies from 0.35 to 1.7 Hz depending on the assumed conditions at the ends of the deck (free deck or constrained deck). At this frequency the motion of the deck seems to be larger than that of the top of the pier for a free deck (the frequency is that of the deck vibrating as a free body on top of the rubber pads). For a constrained deck, the amplitude of the motion of the deck is similar to that of the pier for values of the assumed shear modulus of 6 MPa and 3 MPa but seems to decrease considerably for the value of 1 MPa. As the level of excitation and therefore the level of deformation of the rubber pads increases, the motion of the deck would thus be reduced even at the first natural frequency. Around 6.5 Hz when the deck is constrained and the same motion is applied at the base of all the piers, there seems to be an amplification of the deck's motion for all the values of shear modulus studied.

Comparing the transfer functions for the motion of the deck with that for the case without rubber pads, one can reach the same conclusion. The inclusion of the rubber pads will reduce the motions of the deck over most ranges of frequencies (except perhaps at the fundamental frequency).

If the energy of the earthquake is not around the fundamental frequency of the deck (Chilean earthquakes tend to have predominant frequencies of 3.0 to 4.0 Hz) the effect of the rubber pads on the seismic motions of the deck in the longitudinal direction will be very beneficial. Comparing on the other hand the transfer functions of the motion on the top of pier 4 with and without rubber pads (same figures) it can be seen that the main effect is in the change in the natural frequencies but there is no longer a reduction over most of the frequency range: the amplitudes decrease at the frequencies of the structure without rubber pads and increase instead at the frequencies (more than one) of the structure with rubber pads;

(2) The effect of the rubber pads on the motion of the deck in the transverse direction is less pronounced than in the longitudinal direction. While there are important reductions in amplitude with respect to the top of the pier or with respect to the case without rubber pads, there are now several frequency ranges over which the motion of the deck may be larger than that of the pier (several peaks associated with the motion of the deck);

(3) It appears that the results of the numerical analysis with the model used can explain and reproduce pretty well the main features observed in the recorded data. This includes both the frequencies at which peaks occur and the values of the amplification, although the estimates of the latter could be improved with better estimates of the damping. It should be noticed however that in reality the stiffness of the rubber pads will be varying with time (as the amplitude of the deformation varies). To account for this it would be necessary to conduct nonlinear analyses. A better match of the experimental data would also require more information on the variation of the input motion between the different supports.

Acknowledgments

The authors want to express their gratitude to the Wofford P. Cain Chair at Texas A&M University, and to CONICYT (Consejo Nacional de Investigacion Cientifica y Tecnologica) in Chile, projects 1011025 and 7011025, and the University of Chile in Santiago, Chile, for their financial support that made these studies possible.

References

[1] Skinner RI, Robinson HW, McVerry HC. An introduction to seismic isolation. Chichester (England): Wiley; 1993.
[2] Naeim F, Kelly J. Design of seismic isolated structures: from theory to practice. New York: John Wiley & Sons; 1999.
[3] Turkington DH, Carr AJ, Cooke N, Moss PJ. Seismic design of bridges on lead rubber bearings. Journal of Structural Engineering 1989;115(12): 3000–16.
[4] Chaudhary M. Evaluation of seismic performance of base isolated bridges based on earthquake records. Ph.D. dissertation. Japan: Department of Civil Engineering, University of Tokyo; 1999.
[5] Chaudhary MTA, Abe M, Fujino Y, Yoshida J. System identification of two base-isolated bridges using seismic records. Journal of Structural Engineering 2000;126(10):1187–95.
[6] Chaudhary MTA, Abe M, Fujino Y. Performance evaluation of base-isolated Yama-age bridge with high damping rubber bearings using recorded seismic data. Engineering Structures 2001;23(8):902–10.
[7] Jangid RS. Seismic response of isolated bridges. Journal of Bridge Engineering 2002;9(2):156–66.
[8] Boroschek R, Moroni M, Sarrazin M. Dynamic characteristics of a long span seismic isolated bridges. Engineering Structures 2003;25:1479–90.
[9] Daza VM, Moroni M, Roesset JM, Sarrazin M. Seismic behavior of a bridge with base isolation. In: Proceedings of the 11th NSGCL, 2004.
[10] Segovia ME. (reference of Daza V. M. [12]); 1997.
[11] Romo D. Analisis de registros sismicos y microambientales en el Puente Marga–Marga. Engineering thesis. Santiago, Chile: Civil Engineering Department, University of Chile; 1999.
[12] Daza VM. Interaccion sismica suelo-estructura en el Puente Marga–Marga. Engineering thesis. Santiago, Chile: Civil Engineering Department, University of Chile; 2003.
[13] Latona RW. Analysis of building frames for natural frequencies and natural mode shapes. In: Inter American Program. Cambridge (MA): Civil Engineering Department, MIT; 1969.
[14] Kolousěk V. Dynamics in engineering structures. London: Butterworth; 1973.
[15] Banerjee JR, William FW. Exact Bernoulli–Euler dynamic stiffness matrix for a range of tapered beams. International Journal for Numerical Methods in Engineering 1985;21:2289–302.

[16] Banerjee JR, William FW. An exact dynamic stiffness matrix for coupled extentional-torsional vibration of structural members. Computers and Structures 1994;50:161–6.
[17] Banerjee JR, William FW. Coupled bending-torsional dynamic stiffness matrix for an axially loaded Timoshenko beam element. International Journal of Solids and Structures 1994;31:749–62.
[18] Doyle JF. Wave propagation in structures – an FFT-based spectral analysis methodology. New York: Springer Verlag; 1989.
[19] Doyle JF. Wave propagation in structures – spectral analysis using fast discrete fourier transform. 2nd ed. New York: Springer Verlag; 1989.
[20] Papaleontiou CG. Dynamic analysis of building structures under combined horizontal and vertical vibrations. Ph.D. dissertation. University of Texas, Austin, Texas; 1992.
[21] Gopalakrishnan S, Doyle JF. Wave propagation in connected waveguides of varying cross-section. Journal of Sound and Vibration 1994;175: 347–63.
[22] Yu CP, Roësset JM. Dynamic stiffness matrix for linear members with distributed mass. Tamkang Journal of Science and Engineering 2001;4(4): 253–63.
[23] Dai W. Evaluation of base isolation and soil structure interaction effects on the seismic response of bridges. Ph.D. dissertation. Department of Civil Engineering, Texas A&M University, College Station, TX; 2005.